Available online at www.garmian.edu.krd

Passer Journal of Basic and Applied Sciences

Passer

Passer 7 (Issue 2) (2025) 1053-1063

Original Article

Evaluate the Effect of Drag Force Models on the Fluidization Process

Sherko Ahmad Flamarz Al-Arkawazi*[1]

[1]*Department of Electrical & Computer Engineering, Kalar Technical College, Garmian Polytechnic University, Kalar 46021, Kurdistan Region, Iraq.*

Received 17 July 2025; revised 05 September 2025;
accepted 15 September 2025; available online 29 September 2025

DOI: 10.24271/PSR.2025.535255.2264

ABSTRACT

Drag models are essential the simulation of liquid-solid fluidized beds, a type of multi-phase flow system utilized in various chemical and process industries. Accurate prognosis of the behavior of particles in fluidization is relevant to better performance and efficiency, which allows for accurate predictions regarding pressure decrease and fluidization conditions, i.e., fixed bed, bubbling, turbulent, or homogeneous regimes, are needed, and deeper insight into particle suspension and segregation behavior with possible applications to mixing operations and system stability. Five drag models; Schiller & Naumann model, Dallavalle model, Haider & Levenspiel model, Brown & Lawler model, and Di Felice model are presented, to understand the drag force in terms of its role in governing hydrodynamic behavior during fluidization process, and choose the best probe model. Comparisons between the numerical results for the five models are done; to select appropriate model based on flow regime, porosity, bed height, and particle Reynolds number. The comparisons indicate, the Schiller & Naumann, Dallavalle, and Haider & Levenspiel models exhibit similar trends, in close accord with the experimental findings over the tested extent of velocities. Whereas the Brown and Lawler model tends to underpredict the bed height, particularly at higher inlet velocities. Discrepancy indicates a more conservative estimation drag force on the particle phase, which can lead to less intense fluidization dynamics. The Di Felice model gives the most conservative predictions overall, for the bed height over the velocity range. Selection of appropriate drag force model must correspond to the particular attributes of the fluidized bed stand with the specific characteristics of the fluidized bed under study, which is a liquid-solid fluidized bed.

Keywords: Simulation, Drag models, Fluidization, Multi-phase flow.

1 Introduction

Fluidized beds find extensive applications in powder processing industries because of their high heat and mass transfer rates, and uniform temperature distribution. Fluidized beds applications like; drying, granulation, combustion, gasification, and catalytic reactions involving fine particulate solids. Fluidized particles display three characteristic regions due to an upward fluid: a fixed bed state, a fluidization state, and a thoroughly mixed state [1]. To design, optimize, and scale up fluidized bed reactors efficiently for these applications, it is essential to understand and predict the fluidization behavior of particles over different operating conditions. Particles in fluidized conditions are typically raised and homogenized by a balance between gravitational and drag forces.

Proper modeling of these systems by selecting the right models necessitates capturing the complex particle-fluid interaction, which is dominated by drag forces. Drag force occurs when a body moves through a fluid and pushes the fluid in the direction it is moving. This cause a resistance within the fluid produce reaction force, which is tangential in direction to the motion of the body, is transferred; the drag force experienced in particulate suspensions. Existence a large number of numerical solutions aimed at investigating the interaction between the continuous and particulate phases, the overall picture is still complex to catch.

Several of research studies presenting drag force models have been published, dealed with flow through filters, sedimentation, and fluidization [2-4]. Bed of solid particles in a particulate form can be either bubbling or turbulent, depending on several parameters. Parameters, including particle size, rotational speed, geometry, density, distribution, nozzle shape, ambient pressure and temperature, bed design, and interstitial fluid flow rate, dictate the dynamics of a given system. Primary concerns are concerning particle deformation, since fluid approaching the wall has a highly variable velocity if the bed is intense, along with the definition itself [5]. Accuracy of the classical and more recent drag force models for describing flow in a dilute monodisperse bed is not so well known. To quantitatively evaluate the effectiveness

* Corresponding author
E-mail address sherko.flamarz@gpu.edu.iq (Instructor).
Peer-reviewed under the responsibility of the University of Garmian.

of drag force models, it is crucial to compare simulations with experimental studies of fluidized beds. The powders from Group A, which are fluidized with water, are analyzed through a straightforward drag model, for this purpose three various drag force closure formulations are used: the novel constitutive relation proposed by Mazzei and Lettieri [6], the closure proposed by Wen and Yu [7], and the equation derived from the empirical correlation proposed by Ergun [8]. The variation in drag force models typically demonstrates that the chosen model significantly influences bed expansion, voidage distribution, and mixing dynamics [9]. The Gidaspow model [10] is widely favored due to its effective balance between computational efficiency and precision. Beetstra and Tenneti models [11, 12] offer better fidelity under some conditions but at a higher computational cost [13].

One such research topic is the prediction of fluidization behavior, for intricate systems like fluid-solid systems through simulation based on combined computational fluid dynamics with the discrete element method (CFD-DEM) (multi-phase approach), which is a grid-based approach, coupled with drag force models, and is employed to simulate fluid-solid systems; yet selecting the appropriate drag model remains a critical problem. Combined CFD-DEM has become a standard method for investigating the intricate interactions between fluids and particles at a microscale, thus providing valuable information on flow dynamics, bed properties, and momentum exchange between phases [14,15]. This context, the precision of momentum transfer is governed mainly by the drag force model, which measures the opposition the fluid offered to the particles. Many drag force models have been formulated to explain fluid-solid interactions in fluidized beds. The drag force models applied in this context are designed to predict the drag exerted on the solid phase within a fluidized bed. The fundamental interactions between particles and fluids, as well as interactions among particles themselves, dictate the behavior of solid-fluid systems, which cannot be sufficiently captured by the drag force model. As a result, significant attention is devoted to modeling the drag force experienced by the fluidized bed. A suitable drag model is essential, given that it directly influences primary macroscopic parameters like the bed height (expansion) and particle velocity distribution [16].

Different drag models, as presented in the multi-phase research, are used to investigate the effect of such drag models on bead dynamics in solid-fluid systems [17]. Drag force correlations and their influence on the action of a gas fluidized bed are studied through CFD-DEM simulation [18-20]. An all-encompassing analysis of the interactions among fluids and particles, in addition to the interactions between the particles themselves, is performed by integrating CFD-DEM methodologies [21,22]. Filippo et al. [23] conducted a study that involved comparing various drag force models used in spouted beds through the integration CFD-DEM.

A significant variety of drag correlations have been developed based on experimental, empirical, and semi-analytical principles, each demonstrating different degrees of accuracy across various flow regimes and particle volume fractions. The oldest and most cited correlations includes the Wen and Yu model [7], which is restricted to dilute conditions and might not best describe fluid-particle interactions in denser beds. Sophisticated models, including those by Di Felice [24] and Syamlal-O'Brien [25], account for local porosity and are better applied to dense and heterogeneous fluidized systems. Gidaspow model [10] combines the Wen-Yu and Ergun correlations, adapting itself in response to voidage. It has become increasingly popular in multi-phase simulations for its good balance of accuracy and computational efficiency. Recent advances in CFD-DEM have enabled more comprehensive evaluations of these drag models by directly comparing simulation results with experimental data or high-fidelity simulations. The performance of each model can vary considerably depending on the particle Reynolds number, bed geometry, and particle size distribution [26,27]. It is imperative to evaluate stringently and benchmark drag models in the same simulation framework to determine their applicability and predictive accuracy in liquid-solid fluidized beds.

This study aims to analyze the effect of different drag force models on the hydrodynamics of fluidized beds using a CFD-DEM approach. A systematic analysis of fluidization dynamics, bed expansion, porosity distribution, and particle movement, this work presents a comparative analysis of the impact of five different drag models on results under controlled conditions. The innovation of this research lies in the development of an optimal drag force model for liquid-solid fluidized beds, utilizing a combination CFD-DEM across various inlet liquid velocities. Overall aims of such an integrated approach were: 1) to understand profound influence of drag force in terms of its role in governing hydrodynamic behavior during fluidization process, 2) impact of choosing alternative models of drag in DEM has been evaluated, and 3) to evaluate overall effectiveness of the DEM-CFD integration to simulate the fluidization process accurately.

2 Methods and Materials

In an unresolved CFD-DEM system, the computational fluid dynamics (CFD) divides the domain into finite volumes or cells, treating it as a continuum (Eulerian), while the discrete element method (DEM) accurately represents the solid phase as collections of individual particles, whose mechanics are analyzed using a Lagrangian approach. Forces are exchanged between the two phases, the philosophy of the Eulerian-Lagrangian (coupling approach in CFD-DEM) [28-32].

2.1 Fluid phase

CFD is a numerical tool to study dynamics in a fluid regime of a mixture of gas, liquid, and solids. CFD model originates in conservation of mass and momentum laws, an evolution of the standard theory for mass and motion of continuous phases. Microscopic fluid behavior may be studied with macroscopic descriptors such as velocity, pressure, and temperature solved in a continuum field. Fluid phase is usually treated as a continuum field and described by finding the volume-averaged Navier-Stokes equations, where fluid (liquid) is incompressible and the physical properties (density, viscosity, etc.) are constant. Equations of continuity and momentum are given by;

- Continuity equation:

$$\vec{\nabla}.\vec{u}_f = 0 \tag{1}$$

- Momentum equation:

$$\rho_f\left(\frac{\partial \vec{u}_f}{\partial t} + \vec{u}_f.\vec{\nabla}\vec{u}_f\right) = -\vec{\nabla}p_f + \mu_f\vec{\nabla}^2\vec{u}_f + \rho_f\vec{g} \tag{2}$$

Where the fluid properties are: ρ_f is density, u_f is velocity, p_f is pressure, μ_f is viscosity, and g is gravity.

2.2 Solid phase

The particles are analyzed using the Discrete Element Method (DEM), a numerical model designed to simulate the behavior of individual solid particles. DEM was initially proposed by Cundall and Strack in 1979 [33] to articulate the mechanical dynamics inherent in granular systems. It is presumed that the interaction points among particles are represented as individual points, particularly in the case of spherical forms. When particles traverse a medium, they establish multiple contact points with each other, involving both normal and tangential forces.

Under conditions of fluidization, each spherical particle experiences two primary forces: the buoyant force, which is influenced by the particle's weight, and the drag force from the continuous fluid phase, which acts to bring the system to a state of equilibrium. The magnitude of these forces can be readily altered based on the presence of surrounding fluid, density differences of the two phases, particle size and shape, and flow direction, it is becoming increasingly challenging to predict the fluidization process behavior of the bed numerically.

The particles in a fluidized bed exhibit two types of movement: transitional and rotational, as described by Newton's second law. Therefore, the equation that governs the transitional motion of particle *i* can be described as;

$$m_{p,i}\frac{d\vec{v}_{p,i}}{dt} = \sum_{j=1}^{N}\vec{f}_{c,ij} + m_{p,i}\vec{g} + \vec{f}_{D,i} + \vec{f}_B \tag{3}$$

Where for i^{th} particle, $m_{p,i}$ is the mass, $v_{p,i}$ is the velocity. N is particles number which candidate to touch with particle *i*, $f_{c,ij}$ is the contact force between *i* and *j*, $f_{D,i}$ is the particle *i* and fluid interaction which is coupling CFD-DEM, and f_B is buoyancy force which is expressed by; ($\vec{f}_B = -\rho_f\vec{g}V_{p,i}$), and $V_{p,i}$ is the particle volume.

On the other hand, the governing equation for particle *i* (rolling) can be written as;

$$I_{p,i}\frac{d\vec{\omega}_{p,i}}{dt} = \sum_{j=1}^{N}\left(\vec{T}_{ij}^{t} + \vec{T}_{ij}^{r}\right) + \vec{T}_i^{ext} \quad and \quad I_{p,i} = \frac{2}{5}m_{p,i}R_i^2 \tag{4}$$

Where I is moment of inertia, ω is angular velocity, and R is radius of the particle. $\vec{T}_{ij}^{t}$ is tangential torque, $\vec{T}_{ij}^{r}$ friction torque due to rolling, and $\vec{T}_i^{ext}$ represents all external torques.

2.3 Drag force models

In fluidized beds, drag force is an essential force in the dynamics of fluidized bed. The drag force regulates the strength of the fluid flow that transports solid particles, while also playing a role in maintaining stability within the fluidized bed. Drag force may also be the cause of the difference in the velocity of particles in a fluidized bed, even though all share the same properties of particles, the influence of the surrounding fluid, and the reactor shape. Euler's equations state that the acceleration of a fluid-particle velocity is connected to the pressure gradient of the flow. The drag force on a solid particle is directly connected to the equation of motion of the fluid (Navier-Stokes equation). Drag force is expressed as;

$$\vec{f}_{D,i} = \frac{1}{2}\rho_f C_{D,i}A_{p,i}\left|u_f - v_{p,i}\right|\left(\vec{u}_f - \vec{v}_{p,i}\right) \tag{5}$$

Where $C_{D,i}$ is drag coefficient, and $A_{p,i}$ is the cross-sectional area. Particle Reynolds number is defined as;

$$\text{Re}_{p,i} = \frac{\rho_f\varepsilon_f d_{p,i}\left|\vec{v}_{p,i} - \vec{u}_f\right|}{\mu_f} \quad and \quad \varepsilon_f = \frac{V_{element} - V_{particles}}{V_{element}} \tag{6}$$

Where $d_{p,i}$ is diameter, ε_f is fluid porosity in an element, $V_{element}$ is volume of element, and $V_{particles}$ is volume of all particles in a component. Therefore, it is possible to calculate the porosity of particles from: $\varepsilon_p = 1 - \varepsilon_f$.

Over the years, various drag force models have been developed to characterize such an interactive behavior adequately; nevertheless, most commercially available software-applied drag force models have been understood for almost one century [34]. Several models for drag force include the kinematic drag model, the Schiller & Naumann model, the Dallavalle model, the Haider & Levenspiel model, the Brown & Lawler model, and the Di Felice model. The drag models are chosen cause of their applicability for Reynolds number ranges, and typical uses in CFD-DEM simulations for liquid-solid fluidized beds. Feature of each model can be summarized: 1) Schiller & Naumann is a widely recognized empirical correlation used to calculate drag force on spherical particles within multi-phase flow systems [35]. The model is based on the premise that particles are spherical and that the flow around them is steady. 2) The Dallavalle model is a correction to the Stokes drag law for particle shape factors and high Reynolds numbers [36]. It is applicable when the shape of particles (e.g., elongated or irregular grains) has an essential influence on drag, 3) Haider & Levenspiel proposed a generalized drag coefficient correlation applicable across a broad range of Reynolds numbers (Re = 0.01 to 10,000) [37], which is for irregular or nonspherical particles and more general than Schiller & Naumann, and Dallavalle, 4) Brown & Lawler model includes a drag correction for small, irregular particles, incorporating particle shape and particle-fluid slip effects [38], and extend Schiller-Naumann to include shape corrections, and The Di Felice model is the most popular model used for fluidized bed simulations [24]. It employs a voidage correction to represent particle interactions in dense multi-phase flows, and ideal for fluidized bed and packed bed simulations. Drag coefficients for each model are expressed as;

- The drag coefficient for the Schiller and Naumann model:

$$C_{D,i} = \begin{cases} \frac{24}{\mathrm{Re}_{p,i}}(1+0{,}15\,\mathrm{Re}_{p,i}^{\;0{,}687}) & if \quad \mathrm{Re}_{\mathrm{p,i}} < 1000 \\ 0.44 & if \quad \mathrm{Re}_{\mathrm{p,i}} \geq 1000 \end{cases} \tag{7}$$

- The drag coefficient for the Dallavalle model:

$$C_{D,i} = \left(0.63 + \frac{4.8}{\sqrt{\mathrm{Re}_{p,i}}}\right)^2 \tag{8}$$

- The drag coefficient for the Haider and Levenspiel model:

$$C_{D,i} = \frac{24}{\mathrm{Re}_{p,i}}\left(1+0.186\,\mathrm{Re}_{p,i}^{0.6459}\right) + \frac{0.4251}{1+\frac{8710}{\mathrm{Re}_{p,i}}} \tag{9}$$

- The drag coefficient for the Brown and Lawler:

$$C_{D,i} = \frac{24}{\mathrm{Re}_{p,i}}\left(1+0.15\,\mathrm{Re}_{p,i}^{0.681}\right) + \frac{0.407}{1+\frac{8710}{\mathrm{Re}_{p,i}}} \tag{10}$$

- The drag coefficient for the Di Felice model:

$$C_{D,i} = \left(0.63 + \frac{4.8}{\sqrt{\mathrm{Re}_{p,i}}}\right)^2 \cdot \varepsilon_f^{\;2-\left(3.7-0.65e^{\left(\frac{-(1.5-\log_{10}(\mathrm{Re}_{p,i}))^2}{2}\right)}\right)} \tag{11}$$

The choice of drag force models plays a crucial role in the fluidization behavior predicted through fluidization analysis. Each drag force model is derived from a distinct set of assumptions, selecting of a suitable model needs careful consideration about the particular application of fluidization analysis [1, 39, 40]. Models are compared and assessed in terms of their predictive performances under bubbly, turbulent, poly-disperse, and circulating fluidization conditions using simple and complex numerical methods.

3 Combined CFD-DEM

A highly effective numerical approach for analyzing drag force in fluidization involves the integration CFD-DEM. Investigating of fluid-solid interaction using CFD is a standard numerical method employed to comprehend and solve fluidization problems. The biggest challenges in fluidization research with CFD comes from such complex processes as back mixing, solid mixing, and defluidization, whose complexities cannot be appropriately treated with CFD simulations. The contrary, DEM remains a powerful tool for studying a fluidization system through its ability to simulate individual particles within a system. DEM is utilized to analyze the behavior of individual particles, encompassing their movement and interactions during collisions. However, it is not ideally suited for assessing drag forces that influence the direction of adjacent solid phases [22]. Inconsistencies in the assessment of drag force will significantly impact the final computation results. Consequently, it is advantageous to develop methods for evaluating drag forces using a DEM-CFD simulation model. A result, CFD-DEM integration is increasingly seen to be simulation-led. There is a pressing necessity to combine these methods and introduce new applications to advance research in both academic and commercial settings.

4 Results and Discussions

In systems involving liquids and solids, accurately forecasting hydrodynamic behavior is heavily dependent on the model used for drag force. The drag model determines the resistance faced by a particle, which is influenced by factors such as porosity (voidage within the bed), bed expansion, and stability. Effects of drag force during the fluidization process, in terms of specific variation in drag forces, are examined through the combined CFD-DEM. Such, behavior of drag force in such an integrated CFD-DEM model is examined in detail.

4.1 Validation of the combined CFD-DEM model

The simulations performed in Geldart's D group for 2.0 mm spherical particles have been simulated. Numerical results come from a column with diameter 96 mm and a height 1 m, in which an ascending fluid (water) passes through a spherical particles composed of glass beads (initial height of bed at rest: 100 mm), over a range of inlet water velocities (0.02, 0.06, 0.10, and 0.14 m/s) through the bed. Values of the parameters are shown in Table 1.

Table 1: Physical parameters.

Symbol	Parameter	Value
d_p	Particle diameter (mm)	2.0
ρ_p	Density of glass(kg/m^3)	2450
E	Young's modulus (GPa)	70.0
v	Poisson's ratio (-)	0.35
μ_s	Coefficient of friction, (-)	0.30
e	Coefficient of restitution, (-)	0.90
N	Number of particles (-)	2640
ρ_f	Density of fluid (kg/m^3)	1000
μ_f	Viscosity of fluid (Kg/m.s)	0.001
Δt	Time step (s)	$5*10^{-5}$
t	Simulation time (s)	10.0

4.2 Validation of the drag force models

No universal drag model is ideal for every situation; hence, the choice of model should be determined by factors such as flow regime, solid concentration, and experimental validation. No universal drag model is ideal for every situation; hence, the choice of model should be determined by factors such as flow regime, solid concentration, and experimental validation. Many empirical and semi-empirical models are proposed depending on flow regimes and experimental conditions. In this study, five different models of drag force have been selected from a larger set of available options. The models are Schiller & Naumann, Dallavalle, Haider & Levenspiel, Brown & Lawler, and Di Felice. These models use porosity, Reynolds number, and local solid volume fraction differently, leading to significant differences in their drag predictions in various regimes.

Figure 1 presents the plotting of numerical results for the five models versus experimental findings from literature [40]. Bed is comparatively compact at low velocities, whereas at higher velocities, suspension of particles is appreciably larger, suggesting the development of complete fluidization. Among the models evaluated, the Schiller & Naumann, Dallavalle, and Haider & Levenspiel models exhibit comparable patterns, demonstrating a strong correlation with the experimental data across the velocity range of 0 to 0.14 m/s. In contrast, the Brown & Lawler model tends to slightly underestimate the bed height, particularly at higher inlet velocities. Di Felice model presents the most conservative predictions overall, with a consistent underestimation of the bed height over the velocity range.

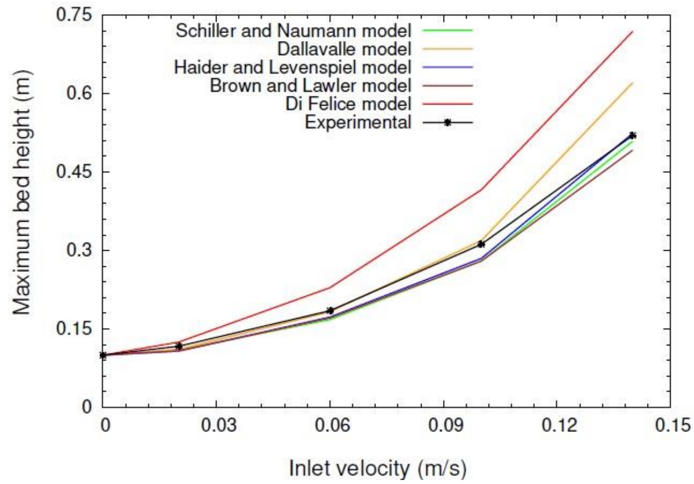

Figure 1: Variation of the maximum bed height with inlet velocity for various drag models with experimental data.

4.3 Comparison of fluid-solid drag force models

Accurate modeling is crucial for forecasting bed hydrodynamics, including aspects like expansion and particle distribution. Drag models provide a mathematical representation of the momentum exchange between the fluid and solid phases. Selection of an appropriate drag model significantly influences the accuracy of CFD-DEM simulations.

Figure 2 shows the time development of bed porosity (voidage) for liquid-solid fluidization. In Figure 2 (a), the porosity increases rapidly from the initial packed-bed condition during the early transient phase (0-2 s) as fluidization begins. Schiller & Naumann, and Dallavalle models yield a quicker increase in porosity than Di Felice, which exhibits higher resistance for dense suspensions. After 2 seconds, porosity oscillations are seen, caused by dynamic interaction between the fluid and particle phases. Oscillations are more dramatic in the Haider & Levenspiel, and Brown & Lawler models because of their complicated Reynolds number.

In Figures 2 (b), 2 (c), and 2 (d), porosity reveals that the porosity for all models raises sharply in the early stage, marking the transition from packed to fluidized conditions. Time development of porosity demonstrates the dynamic behavior of the particle bed during fluidization. All models exhibit an initial rapid expansion of bed porosity, typical of the fluidization onset, as particles move from a packed to a suspended and expanded arrangement. After this transient regime, the porosity tends to level off, which signals the attainment of a quasi-steady fluidized condition. Figure 2 depicts that Schiller & Naumann, and Dallavalle models show similar trends because of their shared reliance on the Reynolds number. In comparison, the models by Haider & Levenspiel, and Brown & Lawler incorporate additional adjustments for particle shape and flow conditions, resulting in a broader range of responses.

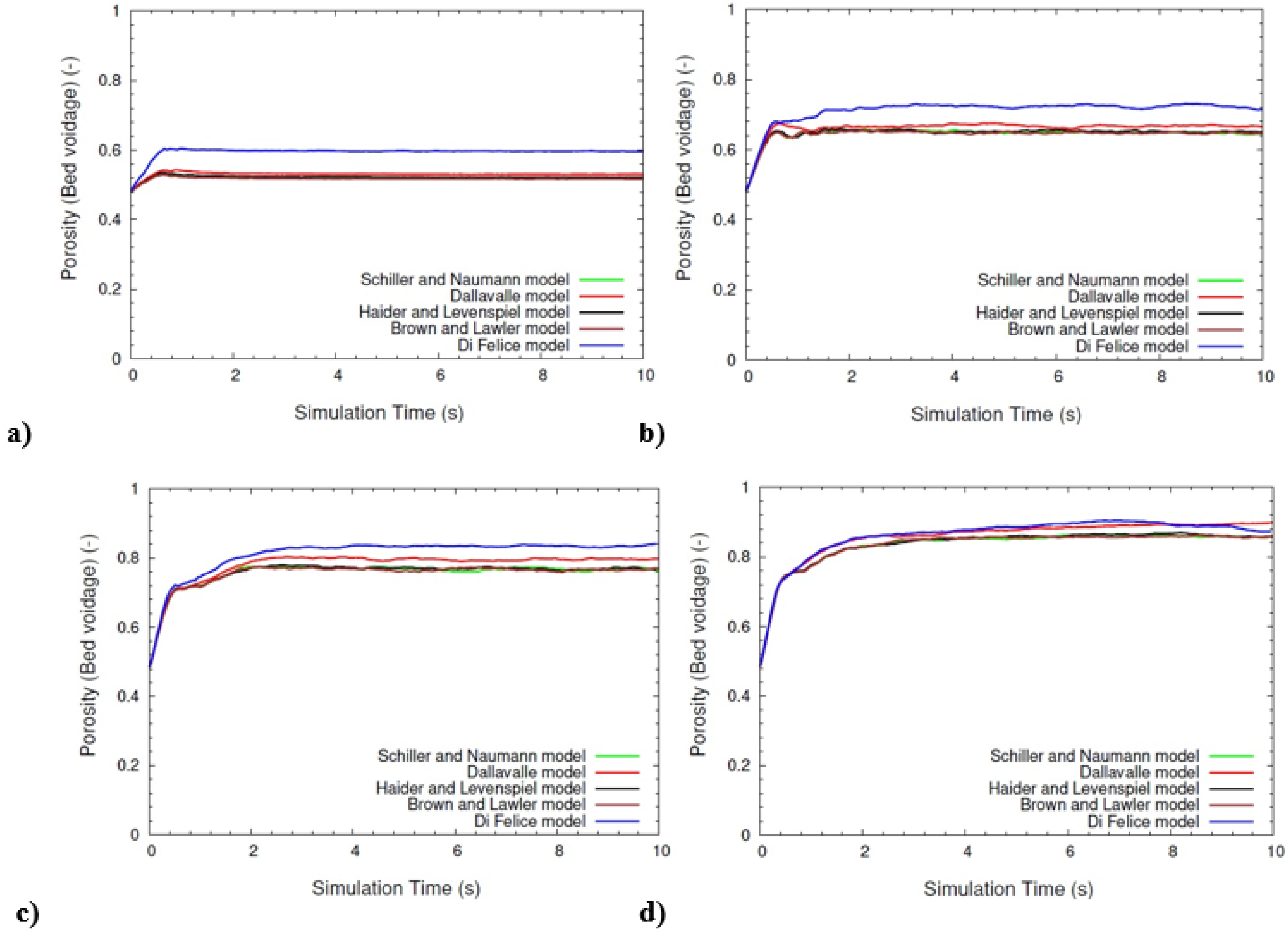

Figure 2: Evolution of bed porosity with time for a range of inlet velocities; a) $v_f = 0.02$ m/s, b) $v_f = 0.06$ m/s, c) $v_f = 0.10$ m/s, and d) $v_f = 0.14$ m/s.

The Figure 2 (d) reveals that, in early period (0-4 s) is marked by temporary particle rearrangements and fast expansion while the liquid phase overcomes the inertia of particles. Past this transient period, the system tends toward a quasi-steady state, where bed height and porosity show small oscillations about mean values. In general, the Schiller-Naumann, and Dallavalle models yield the most stable fluidization profiles, with Haider & Levenspiel and Brown & Lawler showing medium stability, and Di Felice giving the least stable response. This comparison underscores the critical role played by drag formulations in the prediction of the damping of particle motions and the attainment of equilibrium in liquid-solid fluidized beds.

The illustration Figure 3 (a) depicts the initiation of fluidization, indicating that the bed height is significantly influenced by a low inlet water velocity of 0.02 m/s. Bed height was influenced by the velocity of the fluid, as illustrated in Figures 3 (b), 3 (c), and 3(d). In these models, there is a noticeable quick increase in bed height during the first 2 seconds, which aligns with the initial transient acceleration of the fluid and the onset of fluidization. As is apparent, the Di Felice model predicts the highest bed expansion, likely due to its better treatment of particle Reynolds number dependence, which reduces drag for specific flow regimes.

Following the initial transient phase depicted in Figure 3 (d), the bed typically reaches a near-steady state. During this phase, fluctuations in bed height and porosity are minimized, resulting in a stable system in terms of its fluidization characteristics. The Schiller & Naumann, and Dallavalle models are recognized as the most stable among drag models, as both produce smooth porosity-time curves with minimal fluctuations following a quasi-steady state. The medium stability is Haider & Levenspiel, and Brown & Lawler, where slightly higher oscillations are seen due to additional sophistication in their drag corrections. The most unstable among them is Di Felice, as its continuous fluctuations in porosity indicate a tendency to underestimate drag in fluidized conditions.

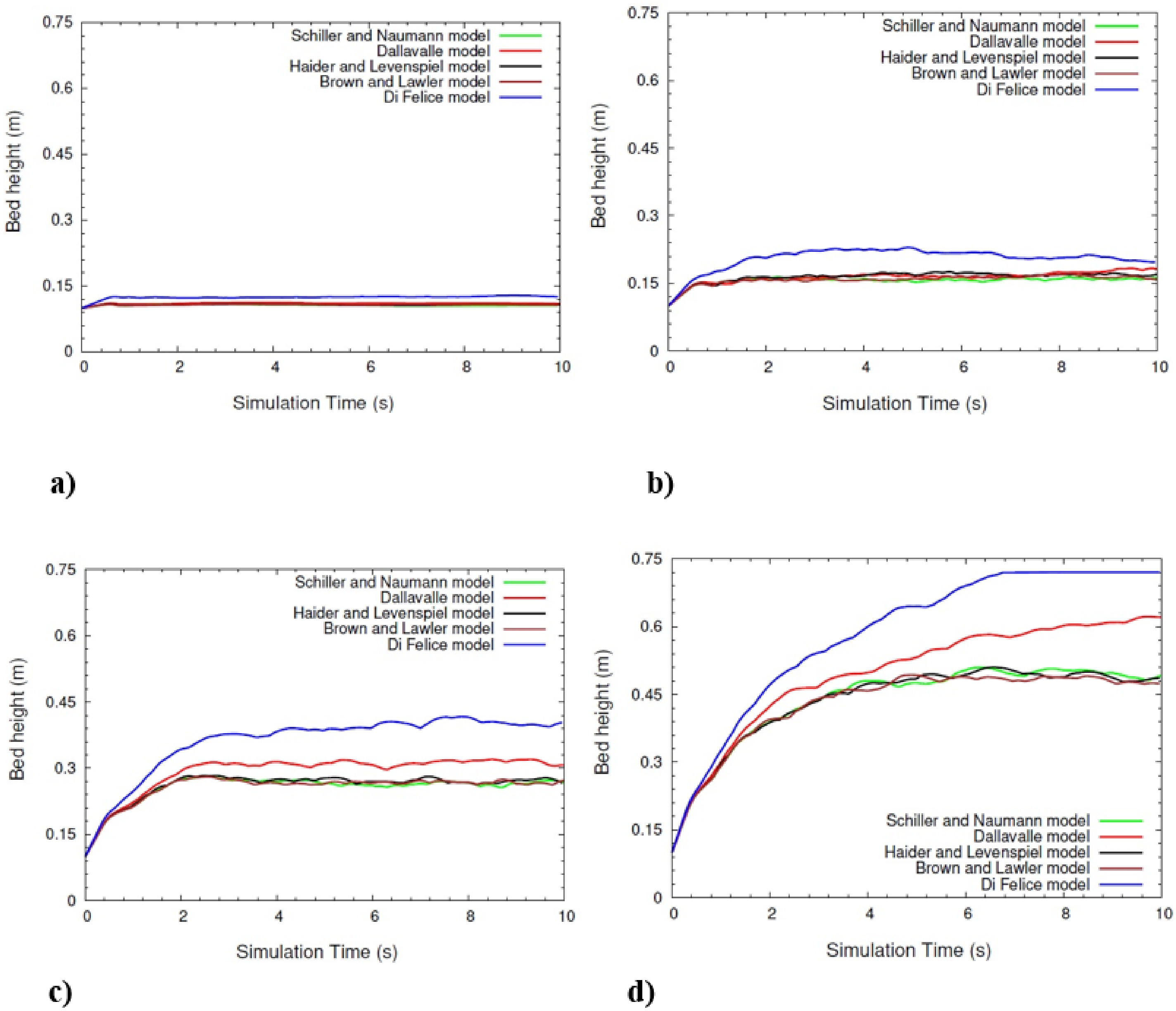

Figure 3: Illustrates variation of bed height with simulation time for a range of inlet water velocities, a) $v_f = 0.02$ m/s, b) $v_f = 0.06$ m/s, c) $v_f = 0.10$ m/s, and d) $v_f = 0.14$ m/s.

In the bottom part of the bed (0-0.15 m) as presented in Figure 4 (a), the porosity is between 0.4 and 0.6, reflecting a densely packed bed caused by high particle concentration. The transition zone, illustrated in Figures 4(b) and 4(c), represents the fluidization interface within the range of 0.15 to 0.45 m, characterized by dominant particle-fluid interactions and noticeable bed expansion. Figure 4 (d) shows the top of the bed (above 0.45 m), which is characterized by a sudden rise in porosity towards values near 0.9. Discrepancy among the models becomes evident here, indicating the sensitivity of CFD-DEM simulations to the choice of drag model. The Schiller & Naumann and Di Felice models yield slightly higher porosity here, reflecting stronger drag forces with earlier mobilization of particles and greater bed expansion. The Dallavalle, and Brown & Lawler models predict lower porosity values, corresponding to a denser bed structure and less fluidization. Haider & Levenspiel model provides intermediate predictions that successfully capture dense and dilute regimes.

The relationship illustrated in Figure 5 between bed porosity and the particle Reynolds number serves as a crucial indicator of fluidization dynamics within liquid-solid systems. At low Re_p presented in Figure 5 (a), all models predict a gradual increase in porosity due to the onset of particle rearrangement and the partial suspension of solids. In this regime, differences between models are minor, with Schiller-Naumann, and Dallavalle showing almost overlapping predictions. This similarity is expected as both models are based on spherical particle assumptions and have comparable formulations at low Reynolds numbers. As the number of repetitions increases, illustrated in Figures 5 (b), 5 (c), and 5 (d), notable differences among the models become clear. Haider & Levenspiel model predicts the highest porosity values; this suggests that Haider & Levenspiel tend to overestimate drag in highly fluidized conditions, leading to larger bed expansions. In contrast, the Brown and Lawler model yields the lowest porosity values, which can be attributed to its primary applicability to fine particles in low Rep regimes, thus underestimating fluidization for larger Re_p. Finally; the Di Felice model exhibits intermediate predictions, with a smooth and realistic porosity evolution across the full Re_p range. This behavior stems from the model's explicit voidage correction term, which accounts for local particle concentration effects and is particularly suitable for dense fluidized beds.

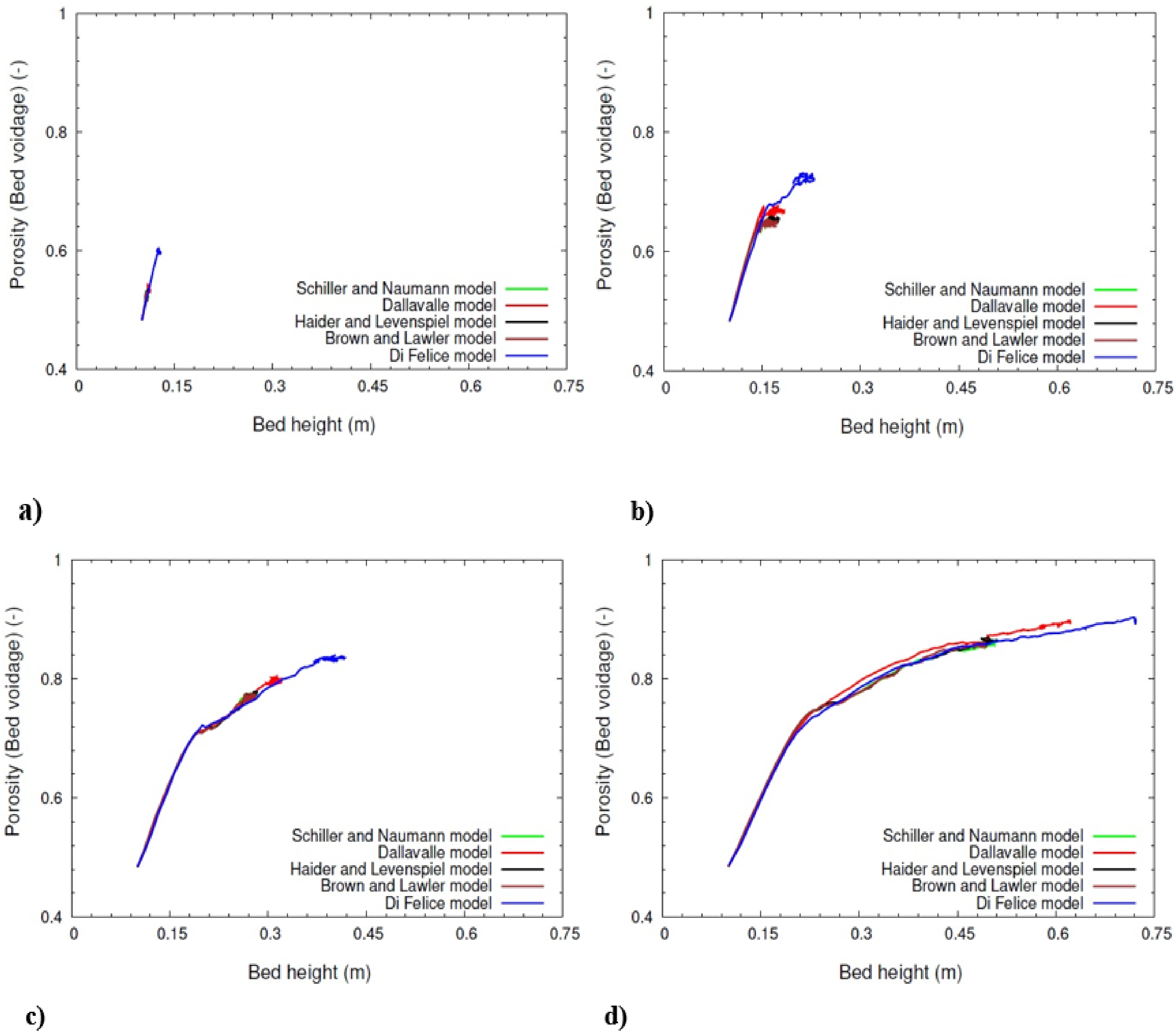

Figure 4: Variation of bed porosity (voidage) as a function of bed height for a range of inlet water velocities, a) $v_f = 0.02$ m/s, b) $v_f = 0.06$ m/s, c) $v_f = 0.10$ m/s, and d) $v_f = 0.14$ m/s.

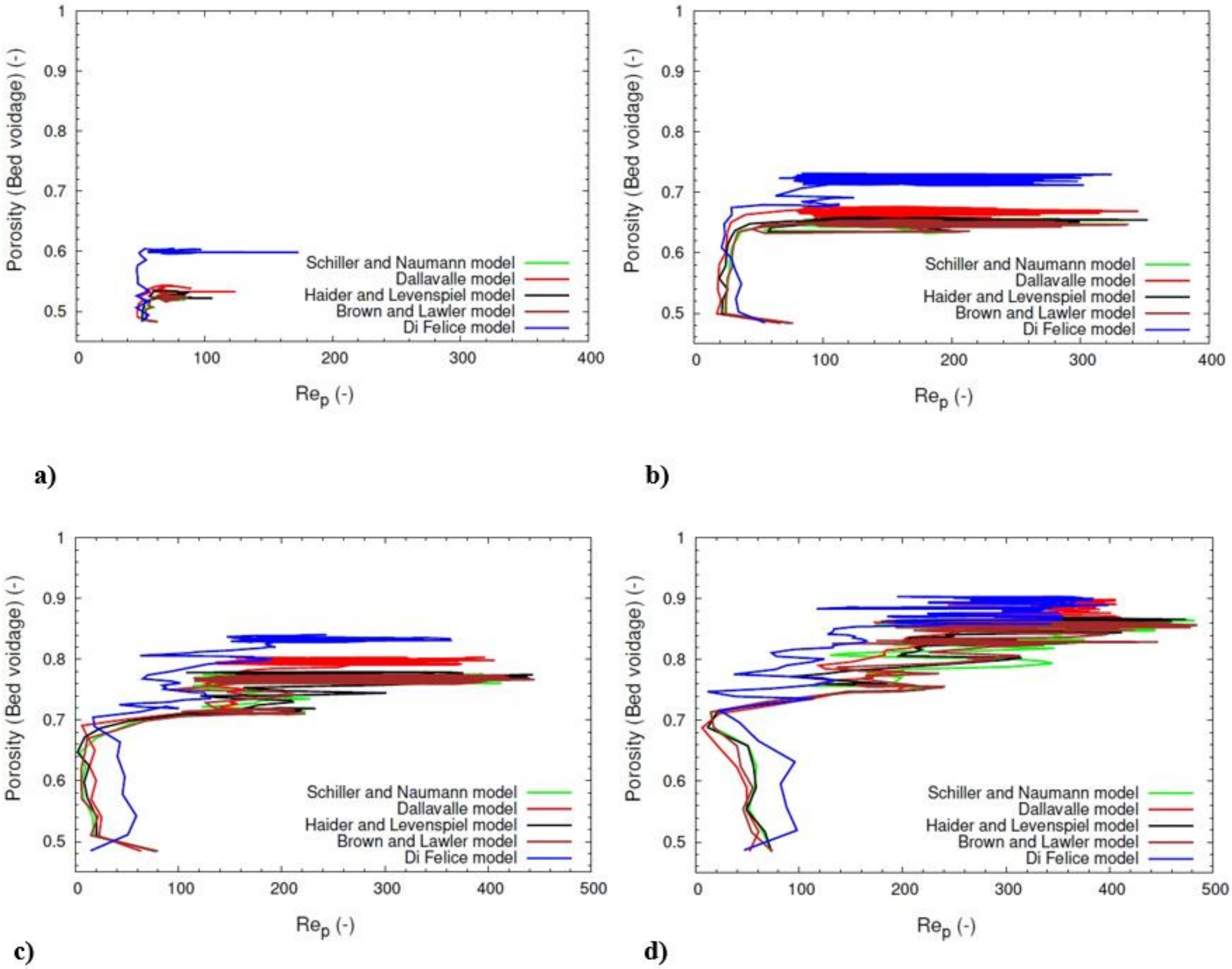

Figure 5: Illustrates variation of porosity with Re_p for a range of inlet water velocities, a) $v_f = 0.02$ m/s, b) $v_f = 0.06$ m/s, c) $v_f = 0.10$ m/s, and d) $v_f = 0.14$ m/s.

In Figure 6, the horizontal axis displays the particle Reynolds number (Re_p), which varies from 0 to 500, while the vertical axis illustrates the dimensionless drag coefficient (C_D). At low Reynolds numbers ($Re_p < 10$), the models converge, reflecting the well-known Stokes flow behavior ($C_D \propto 1/ Re_p$). However, as Re_p increases beyond ~100, notable discrepancies arise; the Schiller & Naumann and Haider and Levenspiel models exhibit a relatively moderate increase in drag, whereas the Brown & Lawler and Di Felice models tend to predict slightly lower drag coefficients at higher Re_p values. Dallavalle model shows intermediate behavior, capturing the transition between regimes. Noted discrepancies at high Reynolds numbers are relevant to fluid-solid interactions, where they are an essential factor in the exchange of momentum, thus affecting the simulation of fluidized beds and particulate transportation.

Conclusions

In this study, the impact of five commonly utilized drag force models Schiller & Naumann, Dallavalle, Haider & Levenspiel, Brown & Lawler, and Di Felice on the hydrodynamics of liquid-solid fluidized beds was thoroughly investigated using a coupled CFD-DEM approach. Among the major conclusions drawn from the comparisons were:

1. Bed height (expansion) and porosity (voidage):

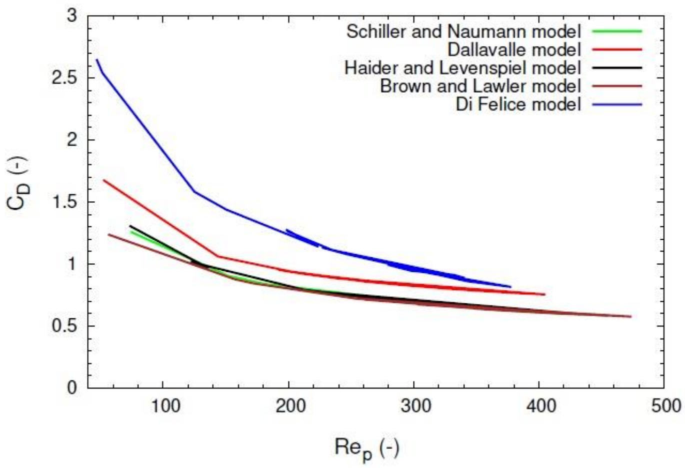

Figure 6: Illustrates C_D versus Re_p for five drag force models for inlet velocity $v_f = 0.14$ m/s.

The Haider & Levenspiel model could predict bed height behavior in intermediate fluidization. The model developed by Brown and Lawler consistently underpredicted bed height at high superficial velocities. The Haider & Levenspiel model's tendency to overestimate porosity may result in inflated rates of mixing and heat transfer in CFD-DEM simulations. Under-prediction, as seen with the Brown and Lawler model, might result in incomplete fluidization and reduced predicted mass transfer rates. The Schiller-Naumann model, while widely utilized, is generally precise only within moderate ranges of replications. For complex systems that include high concentrations of particles, models such as those proposed by Di Felice or Dallavalle are more suitable.

2. Hydrodynamic characteristics:

The Di Felice model better predicted the interphase transfer momentum because it contains a dynamic correction factor including porosity (voidage) dependent drag reduction in packed particle areas. The Dallavalle model featured more drag force fluctuations and introduced differences in the solid circulation patterns.

3. Compatibility of CFD-DEM coupling:

The results emphasize the requirement of selecting appropriate drag models based on the flow conditions and the particle-fluid behavior. According to this research, the Schiller-Naumann and Di Felice models are suggested as the most adaptable models for general liquid-solid fluidization applications. Finally, while all five models are applicable to CFD-DEM simulations, the drag correlation plays a crucial role in determining the fluidization pattern that is predicted. Exploiting the merits of Schiller-Naumann at low Reynolds numbers and the Di Felice at high porosity (voidage) variations might offer improved predictions for large plant-scale liquid-solid fluidized beds.

The variation among models highlights that drag correlations strongly influence bed height (expansion), fluidization onset, and stability. The results of this study shed new light on model-dependent fluidization behavior and highlight the importance of model validation with experimental data, particularly when simulating reactor scales of industrial size. Future extensions of the present work must consider the effect of polydispersity and nonspherical particles, and drag force calibration through data-driven inverse modeling.

Funding

This research received no external funding.

Authors contribution

This research was fully conceived, structured, and carried out by the author. All components of the study, such as data gathering, analysis, and the preparation of the manuscript, were completed independently, guaranteeing a thorough and impartial investigation of the topic.

Conflict of interests

The author of this research state that they have no conflicts of interest with regard to its publication.

References

[1] Osnes, A. N. & Vartda, M. Performance of drag force models for shock-accelerated flow in dense particle suspensions. *Int J Multiphase Flow* **137**, doi:10.1016/j.ijmultiphaseflow.2021.103563 (2021).

[2] Yeoh, G. H. & Tu, J. *In Computational Techniques for Multiphase Flows: Basic and Applications* (2nd ed; Yeoh, G. H., Tu, J., Eds.; Butterworth-Heinemann, 2009).

[3] Norouzi, H. R. *Coupled CFD-DEM Modeling: Formulation, Implementation and Application to Multiphase Flow*. (1st ed.; Wiley: Newark, 2016).

[4] Yang, J. & Renken, A. A generalized correlation for equilibrium of forces in liquid-solid fluidized bed. *Chem Eng J* **92**, 7-14, doi: 10.1016/S1385-8947(02)00084-0 (2003).

[5] Amini, S., Hendrik, C. J., Cloete S., Zaabout A., & Radl S. Evaluation of the minimum fluidization velocity at elevated temperature and pressure through experiments and modeling. *Int Eng Conferences*, (2016).

[6] Mazzei, L. & Lettieri, P. A New Fluid Dynamic Model for the CFD Simulations of Fluidized Beds. *Int. Eng. Conferences, 12th Inter Conference on Fluidization-New Horizons in Fluidization Engineering* (2007).

[7] Wen, C. Y. & Yu, Y. H. Mechanics of fluidization. *Chem Eng Prog Sym Series* **62**,100-11(1966).

[8] Ergun, S. Fluid flow through packed columns. *Chem Eng Prog* **48**, 89-94 (1952).

[9] Tavanashada, V., Passalacqua, A. & Subramaniam, S. Particle-resolved simulation of freely evolving particle suspensions: Flow physics and modeling. *Int J of Multiphase Flow* **135**, 1-12, doi: 10.1016/j.ijmultiphaseflow.2020.103533 (2021).

[10] Gidaspow, D. *Multiphase Flow and Fluidization: Continuum and Kinetic Theory Descriptions*, (Academic Press, 1994).

[11] Beetstra, R., van der Hoef, M. A. & Kuipers, J. A. M. Drag force of intermediate Reynolds number flow past mono- and bidisperse arrays of spheres. *AIChE J* **53**, 2: 489-501, doi: 10.1002/aic.11065 (2007).

[12] Tenneti, S., Garg, R. & Subramaniam, S. Drag law for monodisperse gas-solid systems using direct numerical simulation of flow past fixed assemblies of spheres. *Int J of Multiphase Flow* **37**, 9: 1072-1092, doi: 10.1016/j.ijmultiphaseflow.2011.05.010 (2011).

[13] Gopalakrishnan, P. & Tafti, D. K. Assessment of drag models in fluidized beds using CFD-DEM. *Chem Eng Sci* **127**, 134-147, doi: 10.1016/j.apt.2018.07.014 (2015).

[14] Tsuji, Y., Kawaguchi, T. & Tanaka, T. Discrete particle simulation of two-dimensional fluidized bed. *Powder Technol* **77**, 79-87, doi: 10.1016/0032-5910(93)85010-7 (1993).

[15] Deen, N.G., Van Sint Annaland, M., Van der Hoef, M.A., Kuipers, J.A.M. Review of discrete particle modeling of fluidized beds. *Chem Eng Sci* **62**, 28-44, doi: 10.1016/j.ces.2006.08.014 (2007).

[16] Kuipers, J.A.M., Van Duin, K.J., Van Beckum, F.P.H. & Van Swaaij, W.P.M. A numerical model of gas-fluidized beds. *Chem Eng Sci* **47**, 1913-1924, doi: 10.1016/0009-2509(92)80309-Z (1992).

[17] Mema, I. & T. Padding, J. Fluidization of elongated particles-Effect of multi-particle correlations for drag, lift, and torque in CFD-DEM. *AIChE J* **67**, 1-11, doi: 10.1002/aic.17157 (2021).

[18] Agrawal, V., Shinde, Y., Milinkumar, T. S., Ranjeet, P. U., Vishnu, K. P. & Jyeshtharaj, B. J. Effect of drag models on CFD-DEM predictions of bubbling fluidized beds with Geldart D particles. *Adv Powder Technol* **29**, 11: 2658-2669, doi: 10.1016/j.apt.2018.07.014 (2018).

[19] Varghese, M. M., Vakamalla, T. R., Mantravadi, B. & Mangadoddy, N. Effect of Drag Models on the Numerical Simulations of Bubbling and Turbulent Fluidized Beds. *Chemi Eng Technol* **44**, 5: 865-874, doi: 10.1002/ceat.202000516 (2021).

[20] Ku, X., Li, T. & Løvås, T. Influence of drag force correlations on periodic fluidization behavior in Eulerian-Lagrangian simulation of a bubbling fluidized bed. *Chem Eng Sci* **95**, 94-106, doi: 10.1016/j.ces.2013.03.038 (2013).

[21] Zbib, H., Ebrahimi, M., Ein-Mozaffari, F. & Lohi, A. Comprehensive analysis of fluid-particle and particle-particle interactions in a liquid-solid fluidized bed via CFD-DEM coupling and tomography. *Powder Technol* **340**, 116-130 (2018).

[22] El Geitani, T., Golshana, S. & Blaisa, B. Towards High-Order CFD-DEM: Development and Validation. *Ind Eng Chem Res* **62**, 2: 1-49, doi: 10.1021/acs.iecr.2c03546 (2022).

[23] Marchelli, F., Hou, Q., Bosio, B., Arato, E. & Yu, A. Comparison of different drag models in CFD-DEM simulations of spouted beds. *Powder Technol* **360**, 1253-1270, doi: 10.1016/j.powtec.2019.10.058 (2020).

[24] Di Felice R., The voidage function for fluid-particle interaction systems. *Int J of multiphase flow* **20**, 153-159, doi: 10.1016/0301-9322(94)90011-6 (1994).

[25] Syamlal, M. &O'Brien, T.J. Computer simulation of bubbles in a fluidized bed. *AIChE Symp. Ser.*, **85**,272: 22-31 (1989).

[26] Van Wachem, B.G.M., Schouten, J.C., Van Den Bleek, C.M., Krishna, R. & Sinclair, J.L. Comparative analysis of CFD models of gas-solid fluidized beds. *Chem Eng Sci* **56**, 451-463, doi: 10.1002/aic.690470510 (2001).

[27] Hölzer, A. & Sommerfeld, M. New simple correlation formula for the drag coefficient of non-spherical particles. *Powder Technol* **184**, 361-365, doi: 10.1016/j.powtec.2007.08.021 (2008).

[28] Al-Arkawazi, S., Marie, C., Benhabib, K. & Coorevits, P. Modeling the hydrodynamic forces between fluid-granular medium by coupling DEM–CFD. *Chem Eng Res Des* **117**, 439-447, doi: 10.1016/j.cherd.2016.11.002 (2017).

[29] Esteghamatian, A., Hammouti, A., Lance, M. & Wachs, A. Particle resolved simulations of liquid/solid and gas/solid fluidized beds. *J Phy of Fluids* **29**, doi: 10.1063/1.4979137 (2017).

[30] Al-Arkawazi, S. Simulation the hydrodynamic behavior of binary solid-liquid fluidized beds. *J Mater Environ Sci* **8**, 7: 2522-2529 (2017).

[31] Qinghong Z., Shuyan W., Huilin L., Guodong L., Shuai W. & Guangbo Z. A coupled Eulerian fluid phase-Eulerian solids phase-Lagrangian discrete particles hybrid model applied to gas-solids bubbling fluidized beds. *Powder Technol* **315**, 385-397, doi: 10.1016/j.powtec.2017.04.024 (2017).

[32] Ahmed, A. O., Hussein, E. S., Ahmed, J. S. & Mustafa M. M. A New Formula for Friction Factor-Reynolds Number of Non-Newtonian Fluids, *Passer J basic appl sci* **7,** 2: 698-706, doi: 10.24271/psr.2025.516478.2081 (2025).

[33] Cundall, P.A. & Strack, O.D.L. A Discrete Numerical Model for Granular Assemblies. *Geotechnique* **29**, 47-65 (1979).

[34] Knight, C. Fluid flow and drag in polydisperse granular materials subject to laminar seepage flow. (Imperial College London 2019).

[35] Schiller, L. & Naumann, A. Z. A drag coefficient correlation. Ver. Deut. Ing. **77**, 318-320 (1935).

[36] Dallavalle, J. M., *Micromeritics: the technology of fine particles*. (Pitman Pub. Corp., New York, 1948).

[37] Haider, A., Levenspiel, O. Drag Coefficient and Terminal Velocity of Spherical and Nonspherical Particles. *Powder Technol* **58**, 63-70 (1989).

[38] Brown P., & Lawler D. Sphere drag and settling velocity revisited. *J Envi Eng* **129**, 3: 222–231, doi: 10.1061/(ASCE)0733-9372(2003)129:3(222) (2003).

[39] Flamarz, S. A. Simulating the heat transfer behaviour in a fluidized bed by a combined thermal model in the CFD-DEM coupling, 9th Scientific Conference of University of Garmian, *Special issue for Passer J basic appl sci*, 205-219, doi: 10.24271/PSR.2022.161697 (2022).

[40] Al-Arkawazi S. Simulation the fluidization process by coupling DEM-CFD, *2nd scientific conference*, University of Garmian **2**, (2015).